OPEN

Assessing Fuchs Corneal Endothelial Dystrophy Using Artificial Intelligence–Derived Morphometric Parameters From Specular Microscopy Images

Angelica M. Prada, MD,†‡ Fernando Quintero, BEng,§ Kevin Mendoza, BEng,§ Virgilio Galvis, MD, PhD,*†‡ Alejandro Tello, MD, PhD,*†‡¶ Lenny A. Romero, PhD,‖ and Andres G. Marrugo, PhD§*

Purpose: The aim of this study was to evaluate the efficacy of artificial intelligence–derived morphometric parameters in characterizing Fuchs corneal endothelial dystrophy (FECD) from specular microscopy images.

Methods: This cross-sectional study recruited patients diagnosed with FECD, who underwent ophthalmologic evaluations, including slit-lamp examinations and corneal endothelial assessments using specular microscopy. The modified Krachmer grading scale was used for clinical FECD classification. The images were processed using a convolutional neural network for segmentation and morphometric parameter estimation, including effective endothelial cell density, guttae area ratio, coefficient of variation of size, and hexagonality. A mixed-effects model was used to assess relationships between the FECD clinical classification and measured parameters.

Results: Of 52 patients (104 eyes) recruited, 76 eyes were analyzed because of the exclusion of 26 eyes for poor quality retroillumination photographs. The study revealed significant discrepancies between artificial intelligence–based and built-in microscope software cell density measurements (1322 ± 489 cells/mm^2 vs. 2216 ± 509 cells/mm^2, $P < 0.001$). In the central region, guttae area ratio showed the strongest correlation with modified Krachmer grades (0.60, $P < 0.001$). In peripheral areas, only guttae area ratio in the inferior region exhibited a marginally significant positive correlation (0.29, $P < 0.05$).

Conclusions: This study confirms the utility of CNNs for precise FECD evaluation through specular microscopy. Guttae area ratio emerges as a compelling morphometric parameter aligning closely with modified Krachmer clinical grading. These findings set the stage for future large-scale studies, with potential applications in the assessment of irreversible corneal edema risk after phacoemulsification in FECD patients, as well as in monitoring novel FECD therapies.

Key Words: Fuchs dystrophy, specular microscopy, endothelial cell density, artificial intelligence, deep learning

(*Cornea* 2024;43:1080–1087)

Fuchs endothelial corneal dystrophy (FECD) is a bilateral, progressive disorder characterized by the presence of corneal guttae and loss of corneal endothelial cells.[1,2] Guttae are collagenous protrusions protrusions of the Descemet membrane exerting posterior displacement on the corneal endothelium, and their presence serves as a diagnostic indicator of FECD when observed through slit-lamp biomicroscopy.[3] In early FECD, isolated guttae form in the center of the cornea. Over time, they coalesce and extend, affecting not only the central region but also the peripheral area. In severe cases, this condition can precipitate clinical corneal edema, epithelial bullae, and subepithelial scarring, and may require a corneal transplant.[4]

The progression of FECD is closely tied to endothelial cell dysfunction, stemming from microenvironmental alterations that are, in turn, secondary to changes in the Descemet membrane. These changes include the formation of previously mentioned guttae and modifications in the composition of the extracellular matrix.[5–9] These abnormalities lead to reduction in cell density and alteration in cell morphology, ultimately culminating in further endothelial dysfunction, apoptosis, and, eventually, corneal edema. Although corneas with low endothelial cell densities, up to approximately

Received for publication July 19, 2023; revision received November 1, 2023; accepted November 23, 2023. Published online ahead of print February 9, 2024.

From the *Centro Oftalmológico Virgilio Galvis, Floridablanca, Colombia; †Fundación Oftalmológica de Santander FOSCAL, Floridablanca, Colombia; ‡Facultad de Salud, Universidad Autónoma de Bucaramanga UNAB, Bucaramanga, Colombia; §Facultad de Ingeniería, Universidad Tecnológica de Bolívar, Cartagena, Colombia; ¶Facultad de Salud, Universidad Industrial de Santander UIS, Bucaramanga, Colombia; and ‖Facultad de Ciencias Básicas, Universidad Tecnológica de Bolívar, Cartagena, Colombia.

This work has been partly funded by Ministerio de Ciencia, Tecnología e Innovación, Colombia, Project 124489786239 (Contract 763-2021).

The authors have no conflicts of interest to disclose.

Supplemental digital content is available for this article. Direct URL citations appear in the printed text and are provided in the HTML and PDF versions of this article on the journal's Web site (www.corneajrnl.com).

The authors confirm that all data underlying the findings are fully available without restriction. The final data set and accompanying code are available on the following Open Science Framework repository: https://osf.io/75kmu/ (DOI: 10.17605/OSF.IO/75KMU).

Correspondence: Andres G. Marrugo, PhD, Facultad de Ingeniería, Universidad Tecnológica de Bolívar, Km 1 vía Turbaco, Cartagena 130010, Colombia (e-mail: agmarrugo@utb.edu.co).

500 cells/mm^2, might not initially present changes in visual acuity, determining a critical value of cell count remains unaddressed.[10,11] However, an earlier case report implied that the lowest threshold can fall between 300 and 400 cells/mm^2. Once the cell density drops beyond this range, corneal edema becomes clinically apparent, leading to compromised visual function.[12] This intricate relationship highlights the significance of a comprehensive assessment of endothelial cells for characterizing FECD and gaining a better understanding of its potential clinical implications on visual acuity, both in the short and long term.[13]

Initial clinical classification for FECD was proposed by Krachmer et al[14] and later modified by Louttit et al.[15] However, these classifications suffer from subjectivity and low reproducibility.[16] Recognizing the limitations of these clinical classifications, researchers have explored more sensitive and objective parameters to grade the disease.[16] These include the corneal central-to-peripheral thickness ratio,[16] Scheimpflug corneal optical tomography,[17–19] and anterior segment optical coherence tomography.[20] Despite the valuable insights these methods offer, they primarily focus on edema, rather than changes in endothelial cells, which are ultimately the cause of corneal edema and impaired visual function in FECD.[5,8,21]

Considering the limitations of existing FECD assessment methods that often overlook endothelial cell evaluation, could serve as a clinically relevant tool. However, its utility has been questioned because of limited repeatability, especially exacerbated in the presence of guttae.[5,13,22] Its utility has been questioned because of limited repeatability and the complicating presence of guttae.[19] Yet, advancements in artificial intelligence (AI) offer a potential solution.[23] Specifically, Sierra et al[24] developed an AI approach that automatically differentiates healthy corneal endothelial cells from areas covered by guttae, enabling the calculation of the "effective" endothelial cell density (EECD)[25] and guttae area ratio (GAR%).[25,26]

Building on the advancement made in AI-based FECD assessment by Sierra et al,[24] the aim of our study was to evaluate the clinical relevance of these AI-derived morphometric parameters. We compare them against the established modified Krachmer grading clinical classification (m-Krachmer)[15] to assess their efficacy in providing a more nuanced understanding of FECD.

METHODS

Subjects

This cross-sectional study was conducted at the Centro Oftalmologico Virgilio Galvis and Universidad Tecnologica del Bolivar. Ethical approval was obtained from the Ethics Committees of Fundación Oftalmológica de Santander Carlos Ardila Lulle and Universidad Tecnologica del Bolivar. The study was partially funded by the Ministry of Science and Technology of Colombia (Minciencias). All participants provided written informed consent before their inclusion in the study, in accordance with the Declaration of Helsinki.

Patients were recruited at the Centro Oftalmológico Virgilio Galvis. All participants underwent a comprehensive ophthalmologic evaluation, which included a review of their medical history, self-identified ethnicity assessment, and a slit-lamp examination conducted by an ophthalmologist. Subsequently, patients diagnosed with FECD were included if they met the inclusion criteria, whereas those with other corneal diseases besides FECD or dry eye, as well as those with a history of corneal transplant or cataract surgery, were excluded.

Clinical Grading

After pupil dilation, 2 ophthalmologists captured slit-lamp retroillumination photographs of the corneal endothelium. These photographs were taken from both nasal and temporal sides to ensure comprehensive coverage of the entire cornea, including both central and peripheral areas. This approach follows the methodology outlined by Eghrari et al.[27,28] Subsequently, each ophthalmologist independently classified the photographs using the m-Krachmer clinical grading system for FECD. This grading system, as described by Louttit et al,[15] categorizes FECD into several grades as follows: Grade 0, characterized by the absence of guttae; Grade 1, indicating the presence of 1 to 12 central or paracentral nonconfluent corneal guttae; Grade 2, signifying more than 12 nonconfluent central/paracentral corneal guttae; Grade 3, representing 1 to 2 mm of confluent central/paracentral corneal guttae at the widest diameter of confluence; Grade 4, denoting greater than 2 and up to 5 mm of confluent central/paracentral guttae; and Grade 5, indicating greater than 5 mm of confluent central/paracentral guttae. Grade 6, which involves more than 5 mm diameter of confluent central/paracentral guttae with clinically apparent stromal or epithelial edema, was excluded from our study because of difficulties in capturing endothelial images in such cases.

In this study, some eyes with a grade 0 in m-Krachmer were included because visible central guttae were present in the fellow eye, leading to a diagnosis of FECD. The grading results obtained by both ophthalmologists were compared, and in cases where discrepancies arose, a consensus was reached through discussion.

Specular Microscopy

The study used a Topcon specular corneal endothelial microscope (SP-3000P, Topcon Co, Japan; magnification ×150, and image size of 0.25 × 0.5 mm) to capture a minimum of 4 consecutive photographs (640 × 480 pixels) of the corneal endothelium from each of the following regions: central, inferior, nasal, superior, and temporal. To capture the peripheral zones, patients were instructed to gaze toward the microscope's built-in green light, which varied its position accordingly. Between each image capture, patients were encouraged to rest their eyes and blink. Lubricant eye drops were administered as needed to ensure patient comfort and image clarity.

The microscope's software was set to automatically capture the images. If the software did not provide an image, no manual capture of any zone was attempted, resulting in

a lower number of captured images in certain areas of some eyes. A technician reviewed all images for clarity, and any blurry images were removed, to provide the highest quality data for analysis.

Image Processing and Analysis

Images of the corneal endothelium, from both central and peripheral regions, were processed using the method proposed by Sierra et al.[24] This method uses a convolutional neural network (CNN), an AI method, to produce a robust segmentation of the endothelial cells and guttae. In this study, we used the same CNN weights which were obtained by training with a diverse data set comprising both FECD and non-FECD eyes. Importantly, as validated by Sierra et al,[24] the cell counts produced by this CNN algorithm closely align with ground-truth data prepared by trained ophthalmologists.

Moving on to the specifics of the image processing, the used CNN uses a 5-layer U-Net architecture and takes a specular microscope image as input (Fig. 1A). The output is a distance map which, after a filtering step, produces automatic segmentations for both guttae and healthy cells (Fig. 1B). A region of interest (ROI), marked in red and smaller than the original image, was selected to minimize potential errors due to image artifacts such as blur, shadows, or glare (Fig. 1C). Below are the details of how we selected and defined this ROI.

Centering and Exclusion

The ROI was centered within the specular microscopy microphotograph and excluded the 5 outermost pixels along each of the 4 edges. This reduced the original image's width and height by 10 pixels, resulting in an analysis area of 204 × 428 pixels, approximately equivalent to 238.41 × 500.20 μm (Large-ROI).

Cell Exclusion

To ensure the analysis of complete cells, any cells that were not fully contained within the ROI were excluded. However, all guttae, even if partially within the ROI, were retained because their area is typically larger than that of a single cell (Fig. 1D).

Artifact Handling

When there were image artifacts at the border of the ROI, the dimensions of the ROI were further reduced by 50 pixels in both width and height. This created an area for analysis of 124 × 348 pixels, approximately equivalent to 144.91 × 406.70 μm (Reduced-ROI). Figure 1C illustrates a Reduced-ROI due to a blurry edge in the input image.

As discussed in the previous subsection, we aimed to capture a minimum of 4 consecutive photographs for each corneal region. The parameters for each area were determined based on the median of all obtained parameters calculated from the images, thus addressing local variations in the corneal endothelium. Figure 2 displays additional image acquisitions from the same corneal region of the eye shown in Figure 1, highlighting the benefits of using multiple images to capture regional variations in guttae.

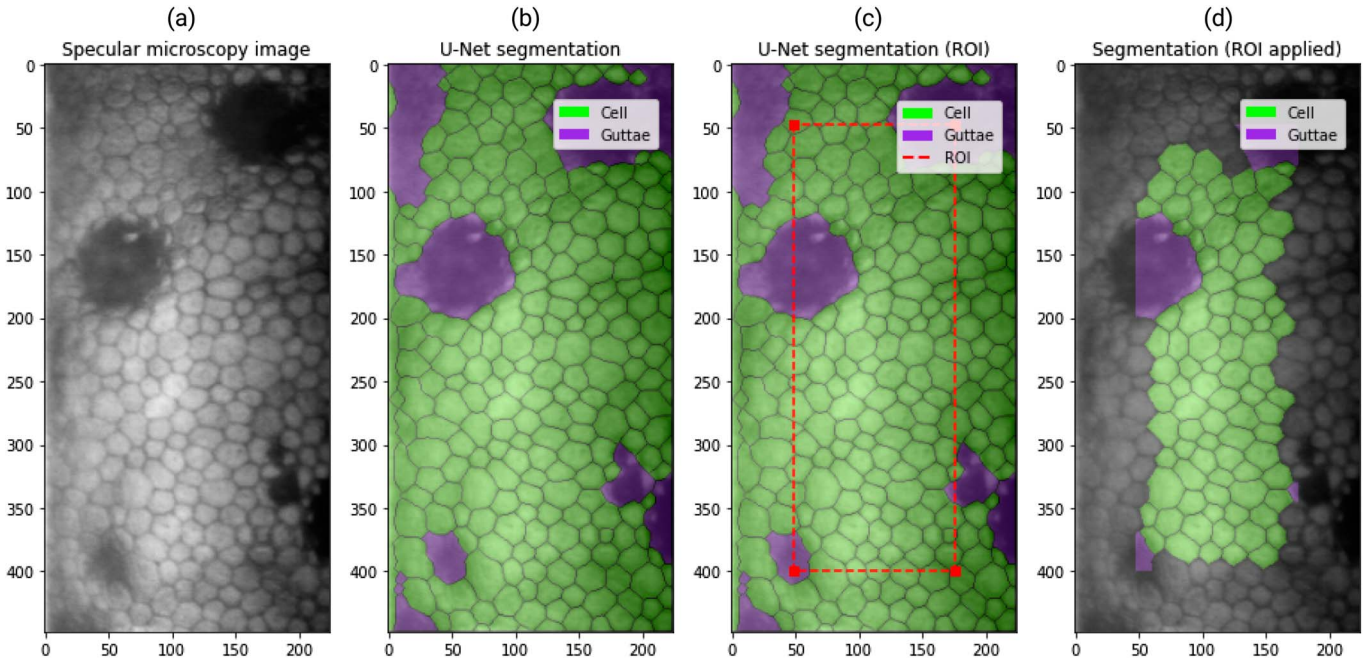

FIGURE 1. A, Original specular microscopy image of the corneal endothelium. B, Segmentation output from the AI-based method, identifying guttae and endothelial cells. C, ROI highlighted by a dotted red line was selected to minimize segmentation errors due to edge artifacts. D, Final segmentation showing only guttae and fully segmented cells within the ROI.

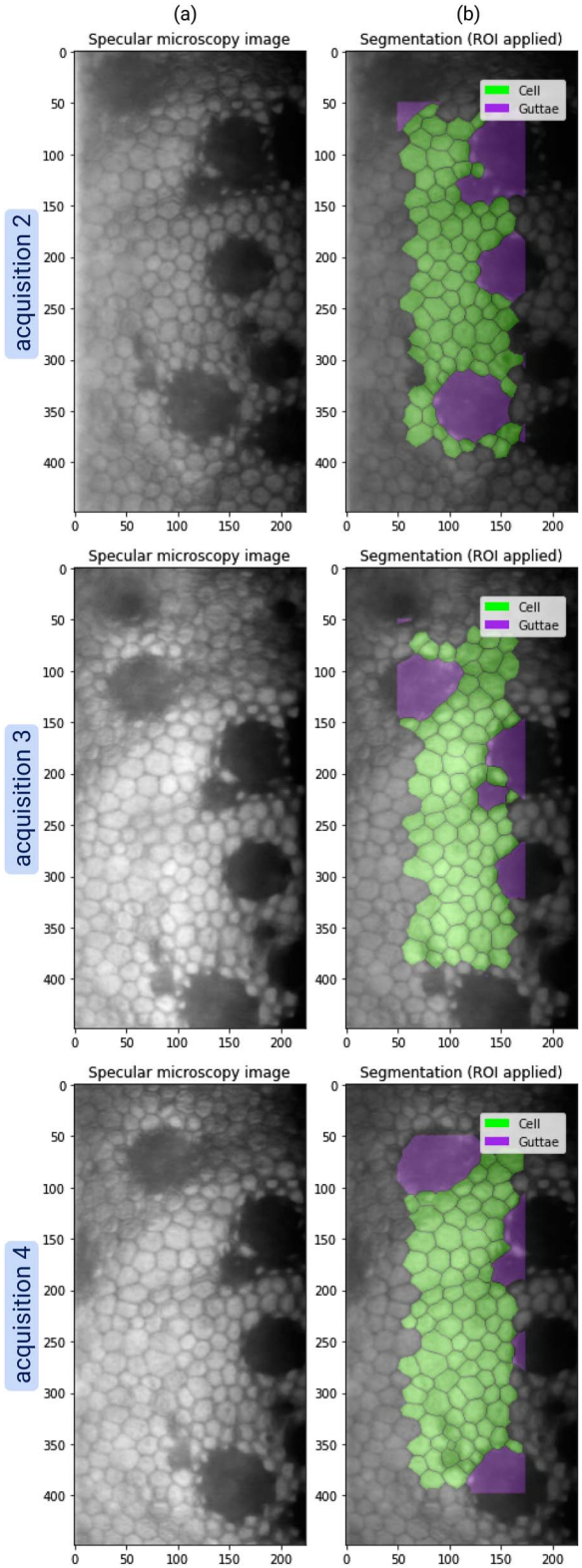

FIGURE 2. Additional images from the same eye and corneal region as Figure 1, illustrating regional variability in guttae distribution, even within a reduced ROI segmentation.

Morphometric Parameters

After applying the mask obtained by specifying the ROI area, we computed the most important morphometric parameters to assess the corneal endothelium: the EECD in cells/mm^2, the coefficient of variation of size (CV%), which is the percentage ratio of the SD of cell area to the average cell area, and the hexagonality in percentage (HEX%). The EECD is the number of cells per unit area, considering in the calculation also the area occupied by guttae, and therefore, it is a value of cell density that is closer to reality in corneal guttata and avoids the overestimation presented by most built-in image analysis software of specular microscopes, which erroneously often exclude the area occupied by the guttae from the calculation. In addition, we calculated and analyzed the new AI-based morphometric parameter recently proposed by Sierra et al,[24] called the "guttae area ratio" (GAR%). To compute this parameter, we used the following equation:

$$\mathrm{GAR}\% = \frac{\text{ROI guttae area}}{\text{ROI segmented area}} \times 100\%,$$

where "ROI guttae area" is the area of guttae regions within the ROI segmented area and "ROI segmented area" is the entire segmented area, including cells and guttae, inside the ROI. This parameter is complementary to EECD and represents the ratio of guttae area (ie, regions without cells or covered by altered cells) to the total analyzed area. This ratio might serve as an indicator of the level of corneal endothelial layer dysfunction, with a higher percentage indicating a greater degree of alteration.

In relation to parameters for guttae assessment, it is important to clarify the distinction between our newly developed GAR% and the existing "R" parameter introduced by McLaren et al.[25] Both aim to quantify the proportion of the corneal endothelium affected by guttae. However, the methodological approach sets them apart. Although "R" relies on manual thresholding for its calculations,[25] GAR% uses an automated CNN to achieve similar ends.[24] This automation eliminates the need for manual intervention, setting GAR% apart as a novel parameter in its approach.

Statistical Analyses

To evaluate the efficacy of AI-based morphometric parameters in characterizing FECD, we conducted the following statistical analyses, considering $P < 0.01$ as the level of statistical significance throughout the study. We calculated median values from the multiple measurements per region to accurately represent the natural variability between images of the same region and to mitigate the effects of outliers. Summary statistics are described as mean and SD unless stated otherwise.

For the initial comparison between the specular microscope software estimated cell density and AI-based effective cell density, we used a *t* test. The variability of m-Krachmer grades between fellow eyes was assessed using an intraclass correlation coefficient (ICC), along with a 95% confidence interval.[29] To further analyze the relationship between

TABLE 1. Number of Images and Eyes per Region

Region	No. Images	No. Eyes
Central	312	76
Inferior	296	74
Superior	210	53
Nasal	253	63
Temporal	300	74

different AI-based parameters and m-Krachmer grades, we adopted a mixed-effects model.[30] This model incorporates the patient identifier as a random effect to account for correlations between eyes from the same patient.

After initial univariate analyses, we used a multivariable mixed-effects model to determine how these parameters collectively predict m-Krachmer grades while also accounting for inter-eye correlation. All variables in the mixed-effects models were standardized using z-score normalization to make them directly comparable, given their different ranges and units. Data analysis was executed in Python 3.9 using Pandas for data handling, SciPy.stats for statistical testing, Pingouin for ICC calculation, statsmodels for fitting the mixed-effects models, and Seaborn for graphical representation.

RESULTS

Patient Details and Overall Outcomes From Specular Microscopy

The 52 patients (104 eyes) included were aged 64 ± 11 years (range 40–85 years). All patients were Colombian from urban areas. Altogether, 14 patients (26.9%) had a family history of FECD. Only 4 patients (7.6%) were male. Three patients (5.7%) had ocular surgery, 1 had an iridotomy, and 2 had laser refractive surgery.

m-Krachmer Clinical Classification

Overall, 26 eyes were excluded because of poor quality retroillumination photographs. Of the 76 remaining eyes subjected to grading, 3 eyes (3.9%) were classified as grade 0 according to the m-Krachmer clinical scale, 6 eyes (7.9%) were grade 1, 20 eyes (26.3%) were grade 2, 13 eyes (17.1%) were grade 3, 20 eyes (26.3%) were grade 4, and 14 eyes (18.4%) were grade 5. The number of specular microscopy images per eye per region is provided in Table 1. Note that only in the central region it was possible to capture at least 3 good quality images for all 76 eyes, whereas in the peripheral regions in several eyes, no analyzable images could be obtained.

Morphometric Parameters

We analyzed a total of 1371 images to calculate the various morphometric parameters. In 84.2% of these images, a Large-ROI was applied for AI-based parameter estimation, whereas the remaining 15.8% used a Reduced-ROI. The mean central cell density calculated by the AI-based approach (EECD) was significantly different from the estimates provided by the built-in software of the specular microscope (1322 ± 489 cells/mm^2 vs. 2216 ± 509 cells/mm^2, $P < 0.001$) reinforcing the need for more advanced measurement techniques for FECD cases that take into account the guttae, as reported by Sierra et al.[24] Comprehensive statistics for the parameters EECD, GAR%, HEX%, and CV% are detailed in Supplemental Digital Content 1 (see Table, http://links.lww.com/ICO/B625).

The ICC strongly indicated that OU of the same patient tend to have similar m-Krachmer grades (0.82, 95% confidence interval of 0.67–0.91). This observation justified our use of mixed-effects models in subsequent analyses, which account for this inter-eye correlation.

Central Region

Table 2 details the univariate correlations between m-Krachmer grades and the AI-based parameters in the central region. Notably, GAR% showed a significant positive correlation with m-Krachmer grades (0.60, $P < 0.001$), as substantiated by Figure 3A, which reveals a marked increase in GAR% between grades 2 and 3. On the other hand, both EECD and HEX% were negatively correlated (−0.37 and −0.36, $P < 0.01$), as visually represented in Figures 3B, C. CV%, however, did not show a statistically significant correlation, as corroborated by Figure 3D.

Peripheral Regions

Although the central region stood out for its strong correlations, we also explored each morphometric parameter in the peripheral regions for a more comprehensive analysis. Among all considered parameters, only GAR% in the inferior region exhibited a marginally significant positive correlation (0.29, $P < 0.05$; Fig. 4B). It is important to note that this result did not meet our predefined alpha level of 0.01 for statistical significance but suggests a trend that may warrant further investigation. By contrast, the other parameters and regions did not yield any statistically significant findings, reinforcing the importance of the central region. The results of univariate correlation for all corneal regions are detailed in Supplemental Digital Content 2 (see Table, http://links.lww.com/ICO/B626).

In summary, the central region consistently exhibited the strongest correlations between the AI-based morphometric parameters and m-Krachmer grades, making it the primary focus for our multivariable mixed-effects regression analysis, as detailed in Table 3. Notably, within the multivariable model that considered all parameters, GAR% emerged as the sole parameter to show a statistically significant positive

TABLE 2. Results of Univariate Correlation of m-Krachmer Grade With the AI-Based EECD, GAR%, HEX%, and CV% Parameters for the Central Region

Parameter	Coefficient	*P*	95% Confidence Interval
EECD	−0.37	<0.01	−0.84 to −0.16
GAR%	0.60	<0.001	0.51–1.12
HEX%	−0.36	<0.01	−0.81 to −0.16
CV%	0.20	0.11	−0.06 to 0.59

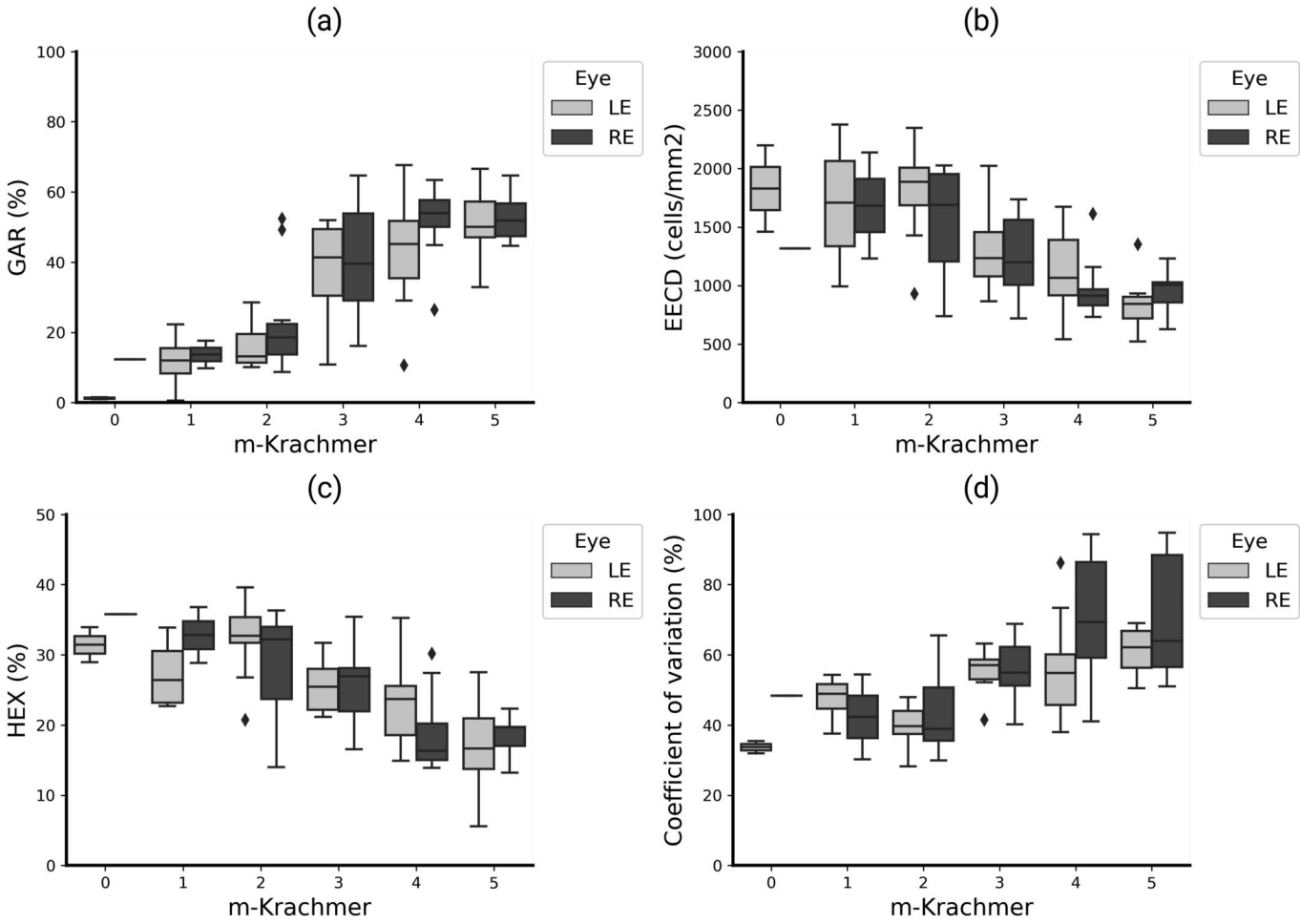

FIGURE 3. AI-based endothelial morphometric parameters compared with FECD m-Krachmer classification in the central cornea. A, GAR%; B, EECD; C, hexagonality; and D, coefficient of variation.

association with m-Krachmer grades (0.86, $P < 0.001$). By contrast, the Group Variance was not statistically significant ($P = 0.163$), indicating that the inclusion of the patient identifier as a random effect had a limited impact when accounting for fixed effects.

DISCUSSION

This study leverages AI, specifically CNNs, for the precise assessment of FECD severity using specular microscopy. The study advances the field by introducing a robust framework that involves precise segmentation and characterization of endothelial cells and guttae for reliable morphometric parameter estimation.

Among the evaluated AI-based morphometric parameters—EECD, CV%, HEX%, and GAR%—GAR% demonstrated the strongest correlation with the m-Krachmer clinical grading for FECD. This aligns with the multifactorial pathophysiology of FECD, which involves not just endothelial cell density but also other factors like guttae and alterations in Descemet membrane.[5,7] In a multivariable regression analysis, GAR% emerged as the most potent predictor of FECD severity, underscoring its potential as a comprehensive clinical metric.

Although our study primarily focused on the central corneal region, we also explored peripheral areas. In the inferior quadrant, GAR% exhibited a marginal correlation, suggesting its potential utility for more comprehensive FECD assessments. This aligns with previous research, which has proposed differential UV light exposure as a contributing factor in FECD progression.[26] Regarding EECD, our study did not yield significant insights into disease progression in peripheral areas. A notable distinction between our research and that of Syed et al[31] is their inclusion of more advanced FECD cases and the use of in vivo confocal microscopy.

Our study had some limitations, including the inability to include corneas with evident edema due to the constraints of specular microscopy. The sample size, although statistically significant, could be expanded in future multicentric studies for more robust validation. Challenges in evaluating retroillumination in some eyes were primarily due to concurrent cataracts. In upcoming investigations, it may be worthwhile to consider incorporating pseudophakic eyes with FECD and clear corneas, a strategy adopted in a recent

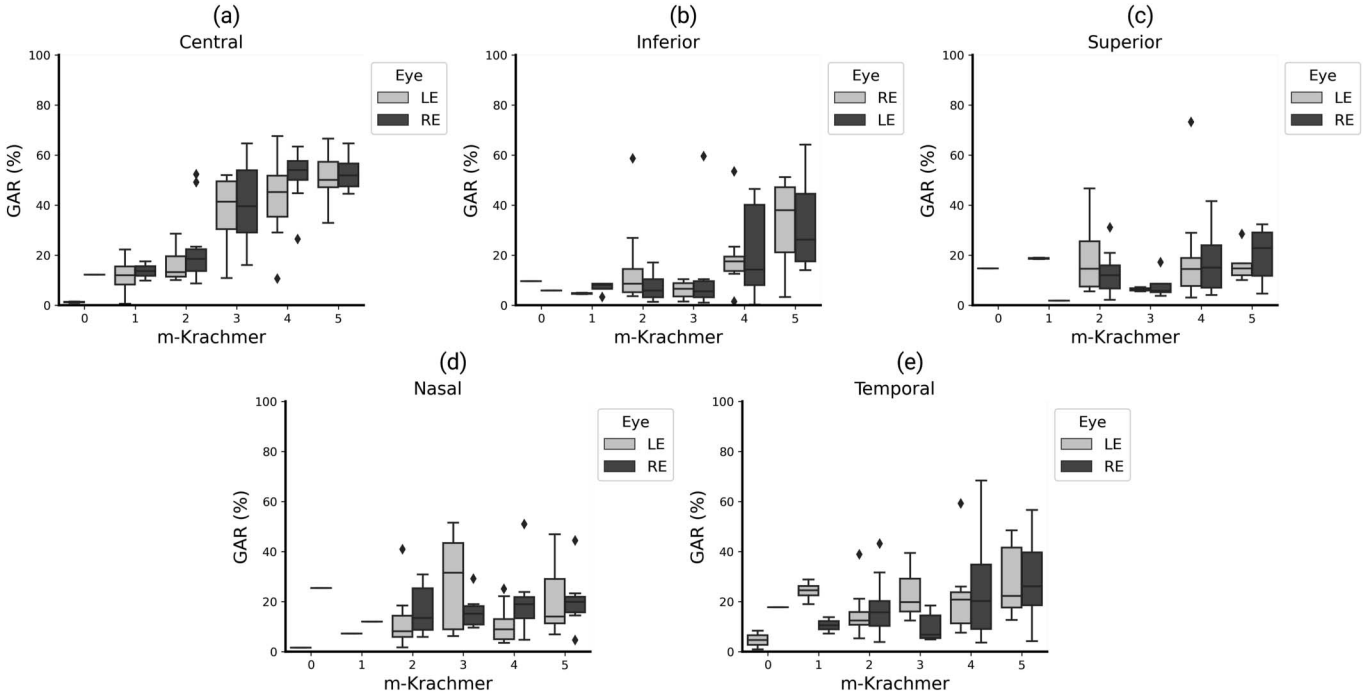

FIGURE 4. GAR% compared with m-Krachmer classification in the central and peripheral corneal zones. A, Central; B, inferior; C, superior; D, nasal; and E, temporal.

study.[9] This would ensure better retroillumination quality during slit-lamp examination.

For technology readiness, the AI system used is in prototype stage, but we have made publicly available the network weights.[32] Although not yet in widespread clinical use, it is poised for future implementation pending further multicentric validation. The system offers more precise FECD assessment, accounting for overlooked metrics related to guttae. Its automated process could also expedite diagnostics, making it more efficient than conventional methods.

In future work, we aim to integrate corneal tomography features and establish precise thresholds for AI-based metrics, both in central and peripheral regions. These advances will enhance our ability to differentiate FECD clinical grades and make more informed clinical decisions, such as the timing of interventions like corneal transplantation. Furthermore, these advances could be instrumental in tracking the effects of novel therapeutics for FECD that may emerge in the near future.[33–35]

TABLE 3. Results of Multivariable Linear Mixed-Effects Regression Model With the AI-Based EECD, GAR%, HEX%, and CV% Parameters in the Central Region

Parameter	Coefficient	*P*	95% Confidence Interval
EECD	0.24	0.23	−0.15 to 0.62
GAR%	0.86	<0.001	0.4007–1.32
HEX%	−0.008	0.96	−0.35 to 0.34
CV%	−0.08	0.53	−0.32 to 0.17
Group Var	0.87	0.16	−0.3527 to 2.0931

CONCLUSIONS

This study underscores the potential of AI, specifically CNNs, in enhancing the objective assessment of FECD with the use of specular microscopy images. Among the evaluated morphometric parameters, GAR% emerged as a significant predictor, aligning closely with the established m-Krachmer clinical grading for FECD. Although our focus was primarily on the central corneal region, GAR% also showed a marginally significant correlation in the inferior peripheral region, hinting at its broader applicability. Although these findings are promising, they serve as a foundation that require further validation through larger multicentric studies. Ultimately, the advancements made in this study could pave the way for more accurate monitoring and therapeutic decision making in FECD, particularly in conjunction with emerging treatments.

ACKNOWLEDGMENTS

This work has been partly funded by Ministerio de Ciencia, Tecnología e Innovación, Colombia, Project 124489786239 (Contract 763-2021). F. Quintero and K. Mendoza thank UTB for a postgraduate scholarship. The authors thank Nicolás Rivero, Rodrigo Piedrahita, and Diego Vega for collaborating in the data-gathering stage. A. G. Marrugo thanks Prof. David Sierra for a discussion on the statistical analysis.

REFERENCES

1. Matthaei M, Hribek A, Clahsen T, et al. Fuchs endothelial corneal dystrophy: clinical, genetic, pathophysiologic, and therapeutic aspects. *Annu Rev Vis Sci*. 2019;5:151–175.

2. Ali M, Cho K, Srikumaran D. Fuchs dystrophy and cataract: diagnosis, evaluation and treatment. *Ophthalmol Ther*. 2023;12:691–704.
3. Margo CE, Espana EM. Corneal endothelial dystrophy. In: Margo CE, Cheng JY, Espana EM, et al., eds. Ophthalmic Pathology: The Evolution of Current Concepts. Cambridge, MA: Academic Press, 2023:147–151.
4. Galvis V, Tello A, Laiton AN, et al. Indications and techniques of corneal transplantation in a referral center in Colombia, South America (2012–2016). *Int Ophthalmol*. 2019;39:1723–1733.
5. Zhang J, Patel DV. The pathophysiology of Fuchs' endothelial dystrophy—a review of molecular and cellular insights. *Exp Eye Res*. 2015;130:97–105.
6. Rodrigues MM, Krachmer JH, Hackett J, et al. Fuchs' corneal dystrophy: a clinicopathologic study of the variation in corneal edema. *Ophthalmology*. 1986;93:789–796.
7. Hribek A, Clahsen T, Horstmann J, et al. Fibrillar layer as a marker for areas of pronounced corneal endothelial cell loss in advanced Fuchs endothelial corneal dystrophy. *Am J Ophthalmol*. 2021;222:292–301.
8. Schrems-Hoesl L, Schrems W, Cruzat A, et al. Cellular and subbasal nerve alterations in early stage Fuchs' endothelial corneal dystrophy: an in vivo confocal microscopy study. *Eye*. 2013;27:42–49.
9. Patel SV, Hodge DO, Treichel EJ, et al. Visual function in pseudophakic eyes with Fuchs' endothelial corneal dystrophy. *Am J Ophthalmol*. 2022;239:98–107.
10. Mishima S. Clinical investigations on the corneal endothelium: XXXVIII Edward Jackson Memorial Lecture. *Am J Ophthalmol*. 1982;93:1–29.
11. Cornea Donor Study Investigator Group, Gal RL, Dontchev M, et al. The effect of donor age on corneal transplantation outcome: results of the cornea donor study. *Ophthalmology*. 2008;115:620–626.e6.
12. Hoffer KJ. Corneal decomposition after corneal endothelium cell count. *Am J Ophthalmol*. 1979;87:252–253.
13. Kocaba V, Katikireddy KR, Gipson I, et al. Association of the gutta-induced microenvironment with corneal endothelial cell behavior and demise in Fuchs endothelial corneal dystrophy. *JAMA Ophthalmol*. 2018;136:886–892.
14. Krachmer JH, Purcell JJ, Young CW, et al. Corneal endothelial dystrophy: a study of 64 families. *Arch Ophthalmol*. 1978;96:2036–2039.
15. Louttit MD, Kopplin LJ, Igo RP, et al. A multicenter study to map genes for Fuchs endothelial corneal dystrophy: baseline characteristics and heritability. *Cornea*. 2012;31:26–35.
16. Repp DJ, Hodge DO, Baratz KH, et al. Fuchs' endothelial corneal dystrophy: subjective grading versus objective grading based on the central-to-peripheral thickness ratio. *Ophthalmology*. 2013;120:687–694.
17. Mingo-Botín D, Arnalich-Montiel F, Couceiro de Juan A, et al. Repeatability and intersession reproducibility of pentacam corneal thickness maps in Fuchs dystrophy and endothelial keratoplasty. *Cornea*. 2018;37:987–992.
18. Patel SV, Hodge DO, Treichel EJ, et al. Predicting the prognosis of Fuchs endothelial corneal dystrophy by using Scheimpflug tomography. *Ophthalmology*. 2020;127:315–323.
19. Sun SY, Wacker K, Baratz KH, et al. Determining subclinical edema in Fuchs endothelial corneal dystrophy: revised classification using Scheimpflug tomography for preoperative assessment. *Ophthalmology*. 2019;126:195–204.
20. Yasukura Y, Oie Y, Kawasaki R, et al. New severity grading system for Fuchs endothelial corneal dystrophy using anterior segment optical coherence tomography. *Acta Ophthalmol*. 2021;99:e914–e921.
21. Aggarwal S, Cavalcanti BM, Regali L, et al. In vivo confocal microscopy shows alterations in nerve density and dendritiform cell density in Fuchs' endothelial corneal dystrophy. *Am J Ophthalmol*. 2018;196:136–144.
22. Ong Tone S, Bruha MJ, Böhm M, et al. Regional variability in corneal endothelial cell density between guttae and non-guttae areas in Fuchs endothelial corneal dystrophy. *Can J Ophthalmol*. 2019;54:570–576.
23. Li Z, Wang L, Wu X, et al. Artificial intelligence in ophthalmology: the path to the real-world clinic. *Cell Rep Med*. 2023;4:101095.
24. Sierra JS, Pineda J, Rueda D, et al. Corneal endothelium assessment in specular microscopy images with Fuchs' dystrophy via deep regression of signed distance maps. *Biomed Opt Express*. 2023;14:335–351.
25. McLaren JW, Bachman LA, Kane KM, et al. Objective assessment of the corneal endothelium in Fuchs' endothelial dystrophy. *Invest Ophthalmol Vis Sci*. 2014;55:1184–1190.
26. Fujimoto H, Maeda N, Soma T, et al. Quantitative regional differences in corneal endothelial abnormalities in the central and peripheral zones in Fuchs' endothelial corneal dystrophy. *Invest Ophthalmol Vis Sci*. 2014;55:5090–5098.
27. Eghrari AO, Garrett BS, Mumtaz AA, et al. Retroillumination photography analysis enhances clinical definition of severe Fuchs corneal dystrophy. *Cornea*. 2015;34:1623–1626.
28. Eghrari AO, Mumtaz AA, Garrett B, et al. Automated retroillumination photography analysis for objective assessment of Fuchs corneal dystrophy. *Cornea*. 2017;36:44–47.
29. Hamlett A, Ryan L, Serrano-Trespalacios P, et al. Mixed models for assessing correlation in the presence of replication. *J Air Waste Manag Assoc*. 2003;53:442–450.
30. Ying G, Maguire MG, Glynn R, et al. Tutorial on biostatistics: statistical analysis for correlated binary eye data. *Ophthalmic Epidemiol*. 2018;25:1–12.
31. Syed ZA, Tran JA, Jurkunas UV. Peripheral endothelial cell count is a predictor of disease severity in advanced Fuchs' endothelial corneal dystrophy. *Cornea*. 2017;36:1166–1171.
32. Sierra J, Pineda J, Volpe G, et al. Code for corneal endothelium assessment in specular microscopy images with Fuchs' dystrophy via deep regression of signed distance maps. GitHub; 2022. Available at: https://doi.org/10.5281/zenodo.7378507.
33. Hemaya M, Hemaya M, Habeeb A. Evaluating keratoplasty for Fuchs' endothelial corneal dystrophy: a literature review. *Cureus*. 2023;15:e33639.
34. Li Z, Duan H, Jia Y, et al. Long-term corneal recovery by simultaneous delivery of hPSC-derived corneal endothelial precursors and nicotinamide. *J Clin Invest*. 2022;132:e146658.
35. Yuan A, Pineda R. Regenerative medicine in Fuchs' endothelial corneal dystrophy. *Taiwan J Ophthalmol*. 2021;11:122–131.